ARCHIVES OF MECHANICS
Arch. Mech. **74** (2-3), 157–172, 2022, DOI: 10.24423/aom.3930

Bödewadt flow and heat transfer of dusty fluid with Navier slip

M. TURKYILMAZOGLU

Department of Mathematics, Hacettepe University, 06532-Beytepe, Ankara, Turkey, e-mail: turkyilm@hacettepe.edu.tr
and
Department of Medical Research, China Medical University Hospital, China Medical University, Taichung, Taiwan

The current work deals with two-phase flow and heat transfer induced by a mixture of fluid and dust particles revolving with a constant angular velocity above a slippage planar wall. Interaction of the solids with the fluid through an interaction force while rotating above the surface is formulated through a similarity system of equations akin to the Bödewadt flow in the absence of suspended particles. Although the velocity fields of fluid and solid are strictly coupled, the heat fields are decoupled from the velocity fields, but they are still in contact with each other due to the coupling of fluid and particle temperatures. The dusty fluid flow character is simulated numerically to capture the fluid and dust phase behaviors. The momentum and thermal layers are resolved in the presence of wall slip mechanism. Illustrative and quantitative results are eventually presented reflecting the physical features of particles and fluid at any stage of interaction during the rotary motion. It is revealed that the wall slip mechanism can be effective enough to alter the usual Bödewadt flow phenomenon.

Key words: revolving flow, velocity slip, dusty fluid, wall shears, fluid-particle interaction, heat transfer.

1. Introduction

Bödewadt flow is one of the classical fluid mechanics problems involving a rotary motion over a planar wall, as physically observed in a well-stirred cup of water [1]. Typical example of particle-fluid suspension in turbine models was mentioned in [2], and some further applications were highlighted in the publications [3–5]. The traditional Bödewadt flow and heat transfer, in which the revolving motion far above a slippage surface is composed of both fluid and solids of equal densities, are the main targets of the present investigation.

The Bödewadt flow accounting for a single fluid was often studied in the literature by some researchers. The response of the finite Bödewadt flow to a harmonic modulation was studied in [6]. Vertical magnetic field influences were reported in [7]. The stability features of the fluid responding to small disturbances were theoretically analyzed in [8]. The absolute and convective in-

stability analysis was made numerically using a spectral method in [9]. The development of boundary layers in fluids between two parallel disks was discussed in [10]. The effects of velocity slip were reported in the Newtonian and non-Newtonian fluids [11, 12]. The potential effects of wall stretching on the flow as well as heat transportation was investigated in [13]. A linear stability analysis was conducted to examine the effect of shear-thinning fluids in Bödewadt flows in [14]. The Bödewadt flow problem in which a nanofluid occupies the space over an infinite disk was explored in [15] considering the Brownian motion and thermophoresis effects. Similarity solutions of the thermal energy problem were shown to exist only for permeable Bödewadt flows in [16]. The porosity effect together with magnetic nanofluid in the presence of geothermal viscosity were considered in [17]. The nonlinear thermal radiation and entropy generation for the Bödewadt boundary layer were carried out in [18].

Two-fluid problems require the balancing of two phases. There are rare works of fluid-particle suspension over the rotating system, such as [19] reporting the effects of suction, [20] examining the impacts of Coriolis and centrifugal forces, [21] exploring the dilute suspension, and [22] searching for the MHD influences. Very recently, inspired by the above studies, [23] has reported the Bödewadt flow with fluid-particle interaction over a standing still surface. When the far-above disk flow revolves against a stretchable rotating disk, a dust phase was found to reduce the velocity and temperature in [24].

The rotating flow problem of fluid-particle interaction has been investigated recently in [23] when the wall slip mechanism impacts are missing. Therefore, the essential motivation here is to complement the latter work by further exploring the velocity slip on the wall and its potential contribution to fluid-particle interaction features. As a consequence, depending on the density distribution taking place within the interaction layer, the inward/outward spiralling of both the fluid and dust phases will be identified. Moreover, the impacts of wall slip on the thermal response of both phases are determined, with potential emphasis upon the heat transfer enhancement.

2. Two phase Bödewadt flow equations

A fluid-particle mixture is supposed to be revolving over a fixed circular plate with a constant angular speed Ω, see Fig. 1. We adopt the cylindrical coordinate system (r, θ, z) and take the fluid velocity field (u, v, w) and particle velocity field (u_p, v_p, w_p), respectively. The wall is fluid-permeable with the wall transpiration

$$w(r, z = 0) = -\sqrt{\nu\Omega}s, \tag{2.1}$$

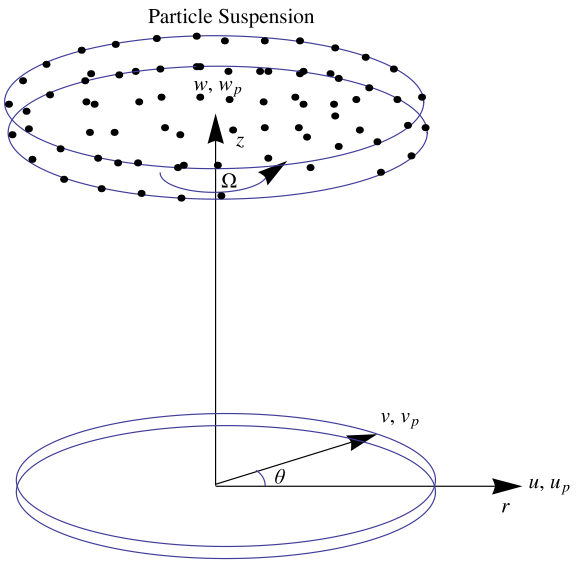

FIG. 1. A configuration showing the two phase flow in the Bödewadt boundary layer.

with $s > 0$ denoting the suction. Also, since the solids are in equilibrium with the fluid revolving at the same rate, we may write:

$$v(r, z \to \infty) = r\Omega, \qquad v_p(r, z \to \infty) = r\Omega. \tag{2.2}$$

Moreover, due to the solid body rotation, the centripetal acceleration in the far field balances the pressure gradient shared by both fluid and particle phases, therefore,

$$p_r = \rho r \Omega^2. \tag{2.3}$$

The radial and axial velocities far above the disk are undisturbed, where the dust particles have the same density ρ_p as that of the fluid ρ, so

$$\begin{aligned} &u(r, z \to \infty) = 0, \qquad u_p(r, z \to \infty) = 0, \\ &w_p(r, z \to \infty) = w(r, z \to \infty), \qquad \rho_p(r, z \to \infty) = \rho(r, z \to \infty). \end{aligned} \tag{2.4}$$

In addition to these, owing to the Navier's fluid slip law at the wall in the radial direction, the wall constraints are:

$$u(r, z = 0) = l u_z(r, z = 0), \qquad v(r, z = 0) = 0, \tag{2.5}$$

where l is the slip coefficient of the fluid phase. As explained in [12], whenever the disk surface has roughness thinner than the boundary layer thickness, in

place of the no-slip condition, the fluid particle can be assumed to have a velocity slip represented by the local shear stress at the wall as above. We should alert that strictly no wall boundary conditions are required for the dust phase, since viscous forces are not needed therein. Because of the fact that the relative motion of dusty flow induces temperature fields T and T_p, respectively for the fluid and particles, we may assume further the constant wall and ambient temperatures, namely:

$$T(r,z=0)=T_w, \quad T(r,z\to\infty)=T_\infty, \quad T_p(r,z\to\infty)=T_\infty. \tag{2.6}$$

Taking into account the axisymmetric fluid and dust conditions, two phase equations for the fluid velocities and temperature are given by [23]:

$$\begin{aligned}
\frac{u}{r}+u_r+w_z &= 0,\\
\frac{u_p}{r}+u_{pr}+w_{pz}+\frac{\rho_{pz}}{\rho_p}w_p &= 0,\\
uu_r-\frac{v^2}{r}+wu_z &= -\frac{1}{\rho}p_r+\nu\left(u_{rr}+\frac{1}{r}u_r+u_{zz}-\frac{u}{r^2}\right)+\frac{\rho_p}{\rho\tau}(u_p-u),\\
u_pu_{pr}-\frac{v_p^2}{r}+w_pu_{pz} &= -\frac{1}{\rho_p}p_r-\frac{1}{\tau}(u_p-u),\\
uv_r+\frac{uv}{r}+wv_z &= \nu\left(v_{rr}+\frac{1}{r}v_r+v_{zz}-\frac{v}{r^2}\right)+\frac{\rho_p}{\rho\tau}(v_p-v),\\
u_pv_{pr}+\frac{u_pv_p}{r}+w_pv_{pz} &= -\frac{1}{\tau}(v_p-v),\\
uw_r+ww_z &= -\frac{1}{\rho}p_z+\nu\left(w_{rr}+\frac{1}{r}w_r+w_{zz}\right)+\frac{\rho_p}{\rho\tau}(w_p-w),\\
u_pw_{pr}+w_pw_{pz} &= -\frac{1}{\rho_p}p_z-\frac{1}{\tau}(w_p-w),\\
uT_r+wT_z &= \frac{\kappa}{\rho c_p}\left(T_{rr}+\frac{1}{r}T_r+T_{zz}\right)+\frac{c_m\rho_p}{c_p\rho\tau}(T_p-T),\\
u_pT_{pr}+w_pT_{pz} &= -\frac{1}{\tau}(T_p-T).
\end{aligned} \tag{2.7}$$

The system (2.7) arises from the usual equations of equilibrium for both fluid and particles phases, and the parameters representing density, kinematic viscosity, thermal conductivity and specific heat are respectively, ρ ν, κ and c_p. It is also taken $c_m=c_p$ for simplicity. Moreover, τ is the relaxation time, from the Stokes drag law. The Stokesian relaxation time for momentum, and that for temperature differs in general, but for the sake of simplicity, they are taken equal in the present analysis. It is also recalled that the difference terms of the

right hand sides of (2.7) are due to the forces and energies representing the particle-fluid interactions.

Benefiting from the von Karman like Bödewadt [1] similarity transformations by means of:

$$
\begin{aligned}
&u = r\Omega F(\eta), \quad v = r\Omega G(\eta), \quad w = (\nu\Omega)^{1/2} H(\eta),\\
&p = -\rho\nu\Omega P(\eta) + \tfrac{1}{2} r\rho^2\Omega^2, \quad T = T_\infty + (T_w - T_\infty)\theta(\eta),\\
&u_p = r\Omega F_p(\eta), \quad v_p = r\Omega G_p(\eta), \quad w_p = (\nu\Omega)^{1/2} H_p(\eta),\\
&T_p = T_\infty + (T_w - T_\infty)\theta_p(\eta), \quad \rho_p = \rho Q(\eta),\\
&\eta = (\Omega\nu^{-1})^{1/2} z,
\end{aligned}
\tag{2.8}
$$

the system (2.7) together with the constraints (2.1)–(2.6) are reduced to

$$
\begin{aligned}
2F + H' &= 0,\\
2QF_p + QH_p' + Q'H_p &= 0,\\
F'' - HF' - F^2 + G^2 + \beta Q(F_p - F) &= 1,\\
F_p^2 - G_p^2 + H_pF_p' + \beta(F_p - F) &= -\frac{1}{Q},\\
G'' - HG' - 2FG + \beta Q(G_p - G) &= 0,\\
2F_pG_p + H_pG_p' + \beta(G_p - G) &= 0,\\
H'' - HH' + P' + \beta Q(Hp - H) &= 0,\\
QH_pH_p' + \beta Q(H_p - H) - P' &= 0,\\
\theta'' - PrH\theta' + Pr\beta Q(\theta_p - \theta) &= 0,\\
H_p\theta_p' + \beta(\theta_p - \theta) &= 0,
\end{aligned}
\tag{2.9}
$$

$$
\begin{aligned}
&F = LF', \quad G = 0, \quad H = -s, \quad \theta = 1 && \text{at } \eta = 0,\\
&F = 0, \quad G = 1, \quad \theta = 0 && \text{as } \eta = \infty,\\
&F_p = 0, \quad G_p = 1, \quad \theta_p = 0 && \text{as } \eta = \infty,\\
&H_p = H, \quad Q = 1 && \text{as } \eta = \infty.
\end{aligned}
\tag{2.10}
$$

The density ratio of fluid and particles is measured by Q in (2.9)–(2.10). The pressure field can be non-trivially obtained after resolving the velocity fields. Equating the two pressure gradient terms in (2.9) enables us to write

$$
QHpH_p' = -H'' - 2\beta Q(H_p - H) + HH', \tag{2.11}
$$

relating the axial components of fluid and particle.

In the reduced system (2.9)–(2.11),

$$\beta = \frac{1}{\Omega\tau} \tag{2.12}$$

is the interaction parameter controlling the two-fluid flow problem,

$$L = l(\Omega\nu^{-1})^{1/2} \tag{2.13}$$

as the velocity slip parameter of the fluid at the wall, and

$$Pr = \frac{\nu\rho c_p}{k} \tag{2.14}$$

is the usual Prandtl number. In the case of $\beta = 0$, we reach the conventional Bödewadt fluid flow problem [12].

We can further define the reduced heat transfer rates of the fluid and particles by

$$Nu_f = -\theta'(0), \qquad Nu_p = \theta_p(0). \tag{2.15}$$

Analogously, the normalized wall shears are

$$-G'(0), \qquad G_p(0) \tag{2.16}$$

and

$$F'(0), \qquad F_p(0). \tag{2.17}$$

In addition to these,

$$-H(\infty) = -H_p(\infty), \tag{2.18}$$

represents the amount of solid/fluid away from the disk.

From (2.12)–(2.18), the interest is with the quantities $F'(0)$, $F_p(0)$, $G'(0)$, $G_p(0)$, $\theta'(0)$, $\theta_p(0)$, $Q(0)$ and $H(\infty)$, which are evaluated with varying physical parameters L, β, s and Pr, respectively. Since we are primarily interested in the effects of wall slip and fluid-particle interaction, we fix s to 2 and Pr to 1, in the subsequent calculations. The studied ranges of L and β are, $[0, 2]$ and $[0, 1.5]$, respectively, though a much vaster range can be recovered. We should recall from the comment in [23] that the impermeable wall has no similarity solutions for the suspended particle problem. Besides, the thermal field receive similarity solution only for non zero values of the suction parameter s [16].

3. Results and discussion

Simulation of system of equations (2.9)–(2.10) is fulfilled by a spectral collocation method based on Chebyshev polynomials. The obtained numerical results were also checked via solving the equations on the Mathematica platform. In order to validate the current physical model, Figs. 2(a–g) are drawn initially in the

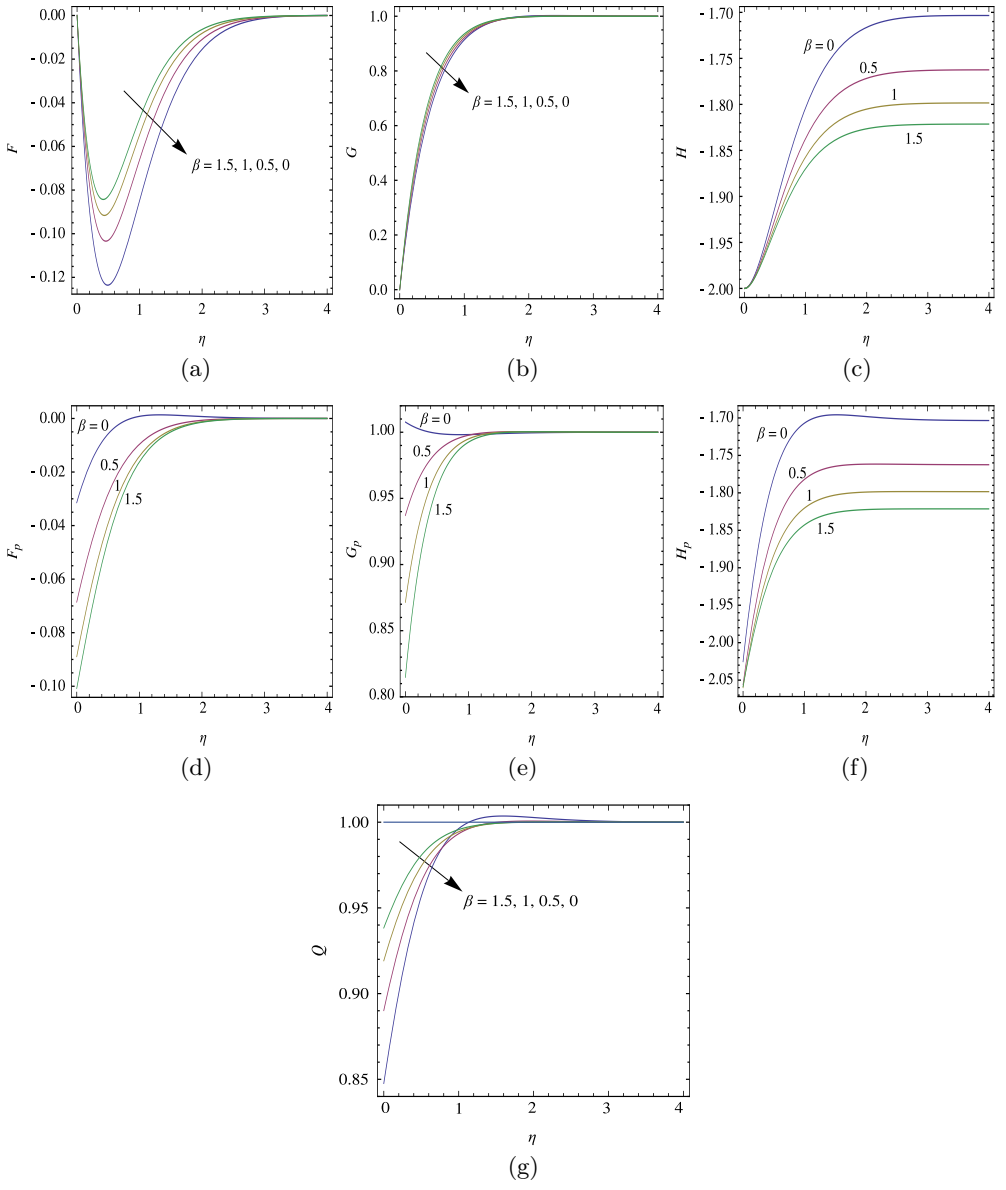

FIG. 2. For the case of no-slip, (a–c) the fluid phase, (d–f) the particle phase and (g) the density ratio.

Table 1. Comparisons with the data in [23] (referring to the succeeding rows) in the case of no-slip.

β	$-F'(0)$	$G'(0)$	$-H(\infty)$	$-F_p(0)$	$G_p(0)$	$-H_p(0)$
0.0	0.64683711	2.15600161	1.70352586	0.03140947	1.00768640	2.02516567
	—	—	—	—	—	—
0.5	0.57689166	2.30374958	1.76248349	.06851471	0.93720578	2.05590190
	0.5770	2.3038	1.7622	0.0685	0.9373	2.0559
1.0	0.53951688	2.43421587	1.79842079	0.08888897	0.87159614	2.05984018
	0.5396	2.4342	1.7983	0.0889	0.8716	2.0599
1.5	0.51917165	2.54527058	1.82139817	0.10075881	0.81490411	2.05844785
	0.5192	2.5453	1.8213	0.1008	0.8149	2.0585

presence of no-slip at the surface. These figures are in full agreement with those presented in [23]. It should be noted that [23] did not consider $\beta = 0$ in their study, for which the fluid and particle phases are decoupled. To verify the present calculations, quantitative results are also tabulated in Table 1, which are in excellent agreement. As concluded in [23], for the no-slip fluid case associated with Figs. 1(a–g), an increase in the fluid-particle interaction parameter leads to less inward spiralling of the fluid phase. In contrast to this, the spiralling is enhanced in the particle phase, with strengthened radial inward and lowered circumferential velocities. To complete the picture as laid down in [23], more comments are required when $\beta = 0$, that is, when the fluid and particles move independently, as two phases are separated. In this special case, more axial movement of the fluid (Fig. 1(c)) is balanced with the more radial displacement of the fluid near the wall (Fig. 1(a)), with diminishing tangential velocity (Fig. 1(b)). As for the dust particles dispersed within the momentum layer, their density distribution varies along the axial direction. Indeed, the absence of particle-fluid interaction gives rise to the lightest distribution of particles proximate to the wall, as clearly visible in Fig. 1(g). To illustrate quantitatively, $Q(0) = 0.847644$ when $\beta = 0$ and $Q(0) = 0.890161$ when $\beta = 0.5$. Such particles near the wall are observed to be revolving with slightly higher angular speed than those at the infinity, refer to Fig. 1(b) and Table 1. Away from the wall in the intermediate layer, particles are denser than the fluid (with increased density ratio $Q(\eta)$), resulting in particles revolving velocity less than unity. Such particles possess the least axial velocities, as seen from Fig. 1(f) and hence a radial outward flow having negligibly small radial velocities occurs, in contrary to the radial inward movement of particles close to the wall. Behavior in the far field of dust particles is in line with that of fluid, since a settlement takes place as the constantly rotating region is approached for fluid and dust phases, in the regime of rigid-body rotation.

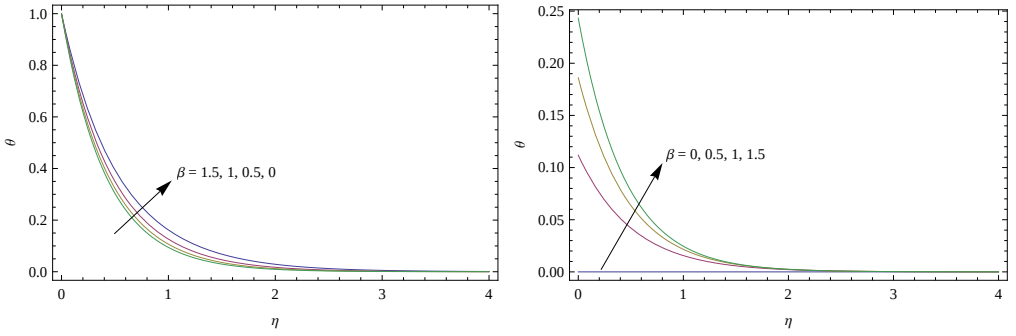

FIG. 3. Temperature profiles of (a) fluid phase and (b) dust phase for $L = 0$.

Figures 2(a, b) are to reveal the thermal behaviors of fluid and dust phases, when the no-slip at the wall applies. It is clear that interaction reduces the temperatures of fluids, whereas it enhances the temperatures of particles. It is remarked that when $\beta = 0$, the fluid has the highest temperature distribution within the thicker thermal layer. On the other hand, temperature of the particles is constant all the way from the infinity up to the wall, when $\beta = 0$. The particle phase encounters a thickening thermal layer, unlike that of a fluid phase. Such a behavior is, no doubt, as a result of a crucial role of the axial velocities of fluid and particle in the associated energy equations. Hence, Figs. 2(a, b) and Table 2 are clear evidences that the interaction cools the fluid, while heating the particles.

Table 2. Fluid heat transfer rate and particle temperature values in the case of no-slip.

β	$-\theta'(0)$	$\theta_p(0)$
0.0	1.91142531	0.00000000
0.5	2.13503044	0.11183009
1.0	2.28978804	0.18606236
1.5	2.41025336	0.24319613

The effects of fluid slip at the wall are next demonstrated in Figs. 3–12. As compared to the no-slip case displayed in Fig. 1(g), the slip mechanism decreases the density ratio next to a surface, where solid particles being lighter than fluid are involved. The influence of slip is appreciably felt with weak interaction, rather than increasing β, refer to Table 3. The mid layer is exposed to dust particles heavier than fluid, whose extend is also increased with an increasing slip parameter.

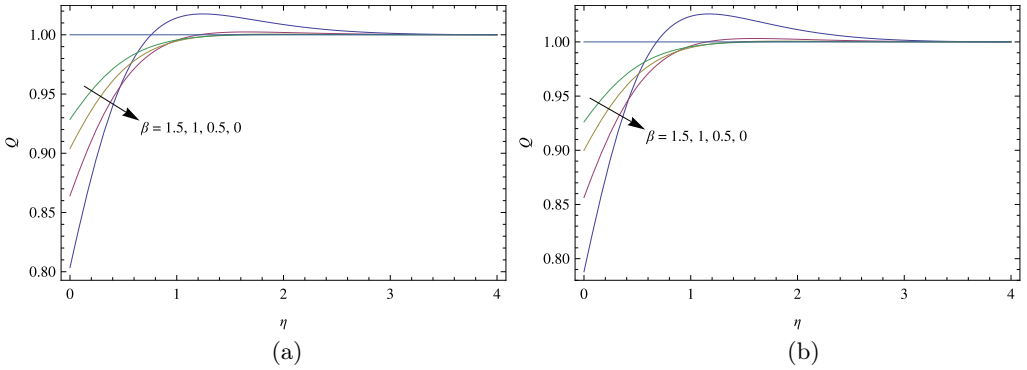

FIG. 4. Evolution of density ratio under slip effect; (a) $L = 1$ and (b) $L = 2$.

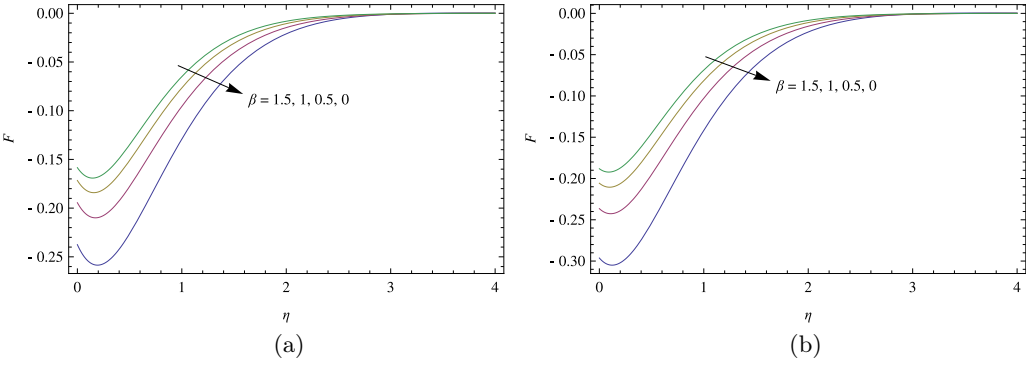

FIG. 5. Radial fluid velocities; (a) $L = 1$ and (b) $L = 2$.

Table 3. Variation of density ratio at the wall.

L	$\beta = 0$	$\beta = 0.5$	$\beta = 1$	$\beta = 1.5$
0	0.84764416	0.89016062	0.91919691	0.93833172
1	0.80348846	0.86407976	0.90391762	0.92855536
2	0.78795419	0.85637980	0.89991546	0.92617494

As far as the fluid phase is concerned, it is witnessed from Figs. 4(a, b) that the velocity slip naturally pushes more fluids in the radial direction with higher speeds by the action of a wall slip mechanism. Not much sensible change is observed in the circumferential velocities of the fluid as compared to Fig. 2(b), with the exception that there occurs a crossover in $G(\eta)$ near $\eta = 1$, see Figs. 5(a, b). This implies that an increasing interaction between the solids and fluid together with the wall slip alters the rotation character of fluid near the wall and away from the wall. This is certainly due to the consequence of mixture distribution shown in Figs. 3(a, b). In comparison with the no-slip axial velocities exhibited

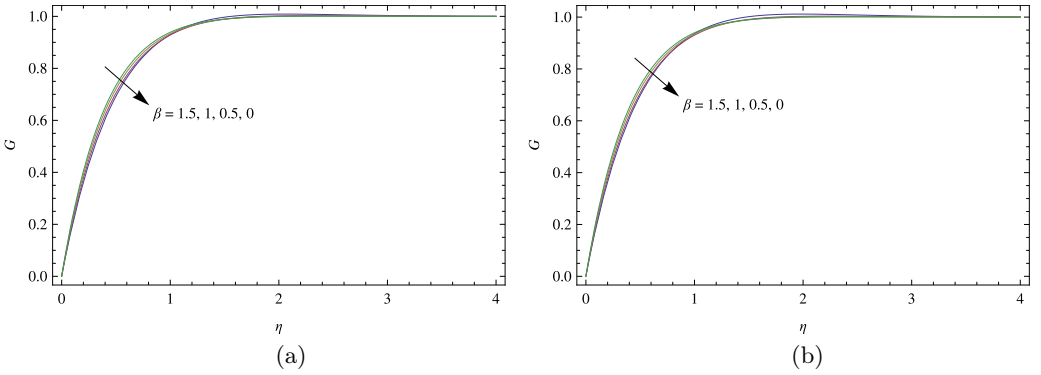

FIG. 6. Tangential fluid velocities;(a) $L = 1$ and (b) $L = 2$.

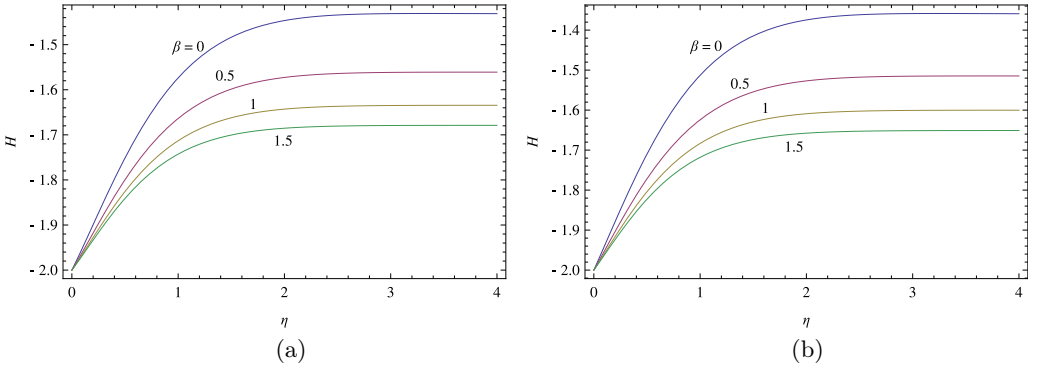

FIG. 7. Axial fluid velocities; (a) $L = 1$ and (b) $L = 2$.

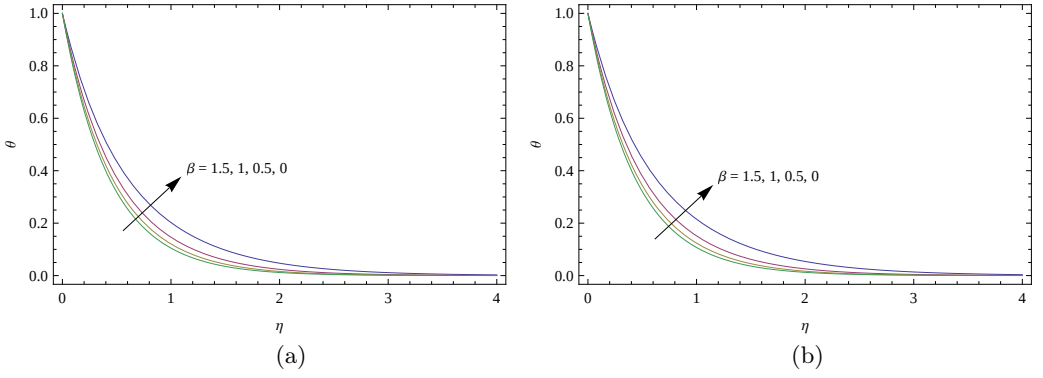

FIG. 8. Fluid temperatures; (a) $L = 1$ and (b) $L = 2$.

in Fig. 2(c), the magnitudes of sucked velocities are dropped when the slip effect is considered as demonstrated in Fig. 6(a, b), also refer to the list in Table 4.

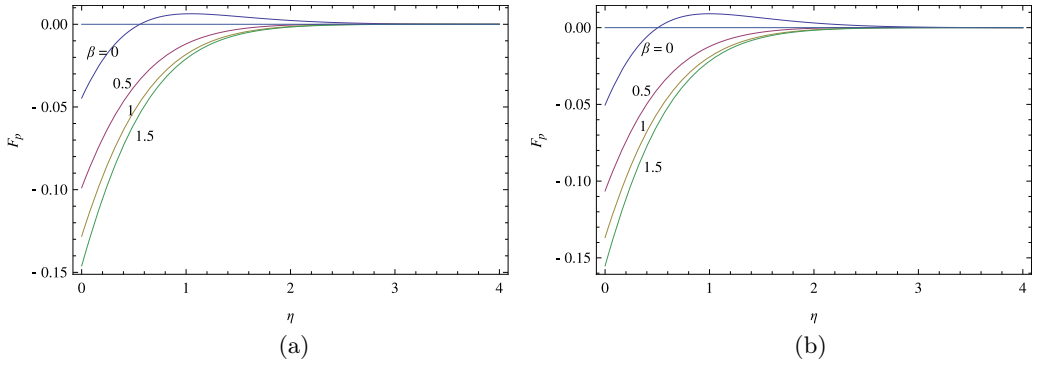

FIG. 9. Radial particle velocities; (a) $L = 1$ and (b) $L = 2$.

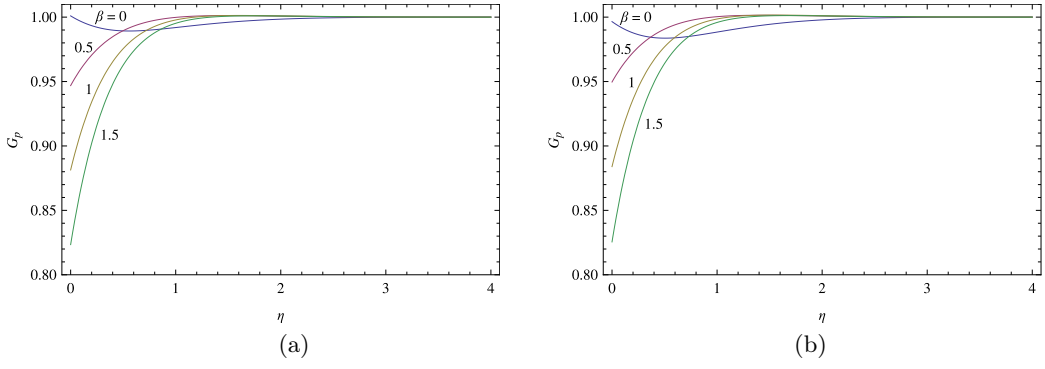

FIG. 10. Tangential particle velocities; (a) $L = 1$ and (b) $L = 2$.

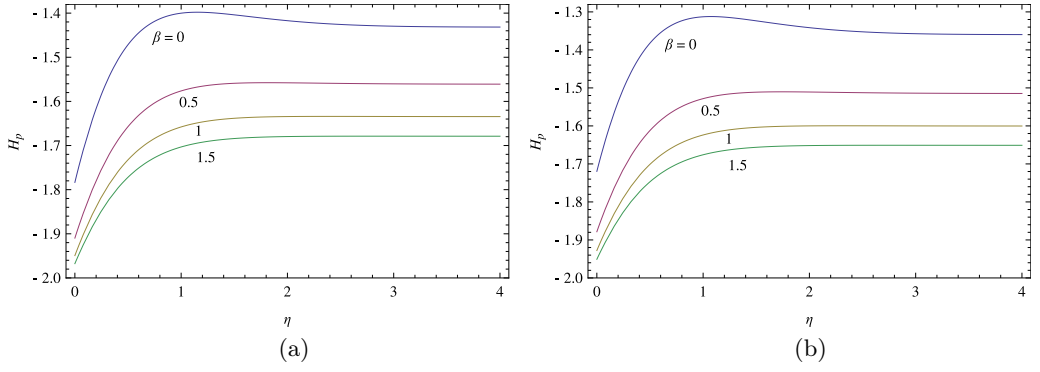

FIG. 11. Axial particle velocities; (a) $L = 1$ and (b) $L = 2$.

In addition to this, profiles are monotonic and the inflectional character of axial velocity is no longer present under the influence of wall slip.

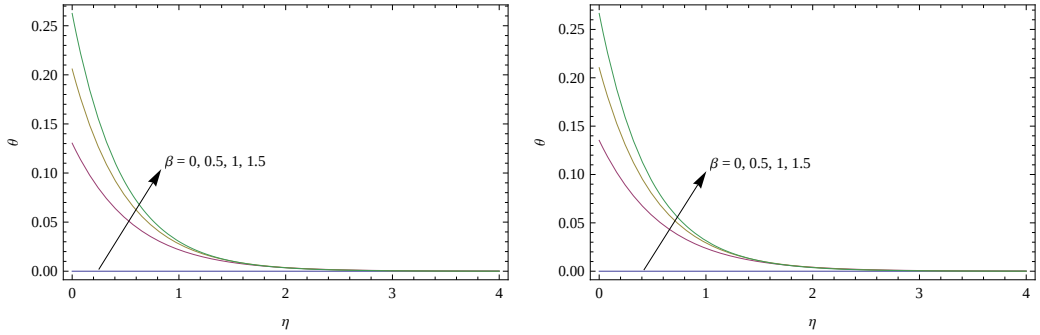

FIG. 12. Particle temperatures; (a) $L = 1$ and (b) $L = 2$.

Figures 7(a, b) indicate that slip increases the temperature profiles by gradually thickening the thermal layer during the fluid phase. Table 4 justifies that slip leads to decrease in the rate of heat transfer at the wall, owing to the heating effect. The slip is also seen to reduce the radial wall shears leading to less drag, as expected [25]. The radial shears are further decreased by the action of interaction. On the other hand, tangential wall shears are enhanced by both slip (less) and interaction (much) mechanisms.

Table 4. Fluid velocity and temperature properties for changing slip parameters.

L	β	$-F'(0)$	$G'(0)$	$-H(\infty)$	$-\theta'(0)$
0	0.0	0.64683711	2.15600161	1.70352586	1.91142531
0	0.5	0.57689166	2.30374958	1.76248349	2.13503044
0	1.5	0.53951688	2.43421587	1.79842079	2.28978804
0	1.5	0.51917165	2.54527058	1.82139817	2.41025336
1	0.0	0.23750746	2.20200353	1.43162670	1.75937273
1	0.5	0.19445671	2.32376296	1.56101755	2.03869279
1	1.5	0.17163557	2.44822751	1.63448410	2.21224880
1	1.5	0.15845967	2.55741215	1.67891940	2.34177489
2	0.0	0.14816311	2.21913731	1.35966570	1.71619029
2	0.5	0.11825758	2.32990200	1.51472604	2.01600191
2	1.5	0.10285817	2.45206646	1.60028097	2.19570303
2	1.5	0.09408281	2.56048765	1.65105118	2.32808598

To gain insight into the velocity field of particle phase, radial velocities are increased in magnitude as for the fluid phase, depicted in Figs. 8(a, b), recall also Fig. 1(d). Due to the distribution of particles close and midway to the wall as previously discussed from Figs. 3(a, b), less interaction gives rise to the backward radial flow. Moreover, weak interaction with an increasing slip parameter causes

the particles next to the wall, revolve at smaller and smaller angular speeds than those at the infinity, as it can be inferred from Figs. 10(a, b). As a result, particle axial velocities are decreased from Figs. 11(a, b), and particle temperatures are increased from Figs. 12(a, b) pronouncedly for weak interactions. Table 5 summarizes the features of particle phase to emphasize the aforementioned physical indications.

Table 5. Particle velocity and temperature properties for changing slip parameters.

L	β	$F_p(0)$	$G_p(0)$	$-H_p(\infty)$	$\theta_p(0)$
0	0.0	0.03140947	1.00768640	2.02516567	0.00000000
0	0.5	0.06851472	0.93720578	2.05590190	0.11183009
0	1.5	0.08888897	0.87159614	2.05984018	0.18606236
0	1.5	0.10075881	0.81490411	2.05844785	0.24319613
1	0.0	0.04463133	1.00097462	1.78350041	0.00000000
1	0.5	0.09883966	0.94684029	1.90973779	0.13037873
1	1.5	0.12818831	0.88136506	1.94940321	0.20592463
1	1.5	0.14610618	0.82341386	1.96764064	0.26254666
2	0.0	0.05043344	0.99652041	1.71956014	0.00000000
2	0.5	0.10644347	0.94963302	1.87846214	0.13530892
2	1.5	0.13676477	0.88395260	1.92786386	0.21042896
2	1.5	0.15526895	0.82551095	1.95095220	0.26655047

4. Conclusions

The classical Bödewadt flow is considered here when the revolving fluid far above a cylindrical wall is interacting with the particles having the same density as the fluid. Hence, the resulting two-phase flow is numerically studied first solving the system of similarity equations. Having resolved the velocity field of fluid and solids, energy equations are also numerically treated to conceive the thermal responses of both fluid and particle phases. The effects of interaction parameter and slip parameter on the physical phenomena can be summarized in the following list:

- When the phases are separate, the fluid moves rapidly downwards with increased radial velocities.
- The density of the mixture drops proximate to the wall, signifying particles lighter than fluid accumulated therein, the lightest occurring without interaction.
- The slip mechanism is more effective on the fluid, but slightly changes the particle phase.

- A region of particles revolving at smaller angular speed than the unity is anticipated by the presence of a wall slip, which implies a radial outward flow contrary to the inward one in the absence of a slip.
- Interaction reduces the fluid temperature, and enhances the particle temperature. Therefore, surface cooling of the fluid is achieved by more interaction.
- A slip leads to thicker thermal layers, and hence heating.

Data availability

The data that support the findings of this study are available from the corresponding author upon reasonable request.

References

1. U.T. Bödewadt, *Die Drehströmung über festem Grunde*, Journal of Applied Mathematics and Mechanics (Zeitschrift für Angewandte Mathematik und Mechanik), **20**, 241–253, 1940.
2. C. Wang, L. Zhang, Z. Li, Z. Gao, J.J. Derksen, *Multi-particle suspension in a laminar flow agitated by a Rushton turbine*, Chemical Engineering Research and Design, **132**, 831–842, 2018.
3. M.T. Montgomery, H.D. Snell, Z. Yang, *Axisymmetric spin-down dynamics of hurricane-like vortices*, Journal of the Atmospheric Sciences, **58**, 421–435, 2001.
4. T. von Larcher, P.D. Williams, *Modeling Atmospheric and Oceanic Flows: Insights From Laboratory Experiments and Numerical Simulations*, John Wiley & Sons, London, 2014.
5. M. Turkyilmazoglu, *Magnetohydrodynamic two-phase dusty fluid flow and heat model over deforming isothermal surfaces*, Physics of Fluids, **29**, 013302, 2017.
6. Y. Do, J.M. Lopez, F. Marques, *Optimal harmonic response in a confined Bödewadt boundary layer flow*, Physical Review E, **82**, 036301, 2001.
7. P.A. Davidson, A. Potherat, *A note on Bödewadt–Hartmann layers*, European Journal of Mechanics B/Fluids, **21**, 545–559, 2002.
8. S.O. MacKerrell, *Stability of Bödewadt flow*, Philosphical Transactions of the Royal Society of London, Series A, Mathematical, Physical and Engineering Sciences, **363**, 1181–1187, 2005.
9. H.A. Jasmine, J.S.B. Gajjar, *Absolute instability of the von Karman, Bödewadt and Ekman flows between a rotating disc and a stationary lid*, Philosophical Transactions of the Royal Society, Series A: Mathematical, Physical and Engineering Sciences, **363**, 1131–1144, 2005.
10. K.M.P. van Eeten, J. van der Schaaf, J.C. Schouten, G.J.F. van Heijst, *Boundary layer development in the flow field between a rotating and a stationary disk*, Physics of Fluids, **24**, 033601, 2012.

11. B. SAHOO, S. PONCET, *Effects of slip on steady Bödewadt flow of a non-Newtonian fluid*, Communications in Nonlinear Science and Numerical Simululation, **17**, 4181–4191, 2012.

12. B. SAHOO, S. ABBASBANDY, S. PONCET, *A brief note on the computation of the Bödewadt flow with Navier slip boundary conditions*, Computers and Fluids, **90**, 133–137, 2014.

13. M. TURKYILMAZOGLU, *Bödewadt flow and heat transfer over a stretching stationary disk*, International Journal of Mechanical Sciences, **90**, 246–250, 2015.

14. M.A. ABDULAMEER, P.T. GRIFFITHS, B. ALVEROGLU, S.J. GARRETT, *On the stability of the BEK family of rotating boundary-layer flows for power-law fluids*, Journal of Non-Newtonian Fluid Mechanics, **236**, 63–72, 2016.

15. J.A. KHAN, M. MUSTAFA, T. HAYAT, F. ALZAHRANI, *Numerical study for Bödewadt flow of water based nanofluid over a deformable disk: Buongiorno model*, Indian Journal of Physics, **91**, 527–533, 2017.

16. M. RAHMAN, H.I. ANDERSSON, *On heat transfer in Bodewadt flow*, International Journal of Heat and Mass Transfer, **112**, 1057–1061, 2017.

17. J.V. KUMAR, R. PARAS, S.R. KUMAR, T. DHARMENDRA, *Porosity effect on the boundary layer Bödewadt flow of a magnetic nanofluid in the presence of geothermal viscosity*, The European Physical Journal Plus, **132**, 2017.

18. M. MUSTAFA, I. POP, K. NAGANTHRAN, R. NAZAR, *Entropy generation analysis for radiative heat transfer to Bödewadt slip flow subject to strong wall suction*, European Journal of Mechanics, B/Fluids, **72**, 179–188, 2018.

19. K.K. SANKARA, L.V.K.V. SARMA, *On the steady flow produced in fluidparticle suspension by an infinite rotating disk with surface suction*, International Journal of Engineering Science, **23**, 875–886, 1985.

20. J.P. TANZOSH, H.A. STONE, *Motion of a rigid particle in a rotating viscous flow: an integral equation approach*, Journal of Fluid Mechanics, **215**, 225–256, 1994.

21. M.R. FOSTER, P.W. DUCK, R.E. HEWITT, *The unsteady Karman problem for a dilute particle suspension*, Journal of Fluid Mechanics, **474**, 379–409, 2003.

22. S. MANJUNATHA, B.J. GIREESHA, C.S. BAGEWADI, *Series solutions for an unsteady flow and heat transfer of a rotating dusty fluid with radiation effect*, Acta Mathematica Universitatis Comenianae, **86**, 111–125, 2017.

23. M. RAHMAN, H.I. ANDERSSON, *Heat and fluid flow in revolving fluid-particle suspensions with suction*, Computational Thermal Sciences, **12**, 417–428, 2020.

24. M. TURKYILMAZOGLU, *Suspension of dust particles over a stretchable rotating disk and two-phase heat transfer*, International Journal of Multiphase Flow, **127**, 103260, 2020.

25. T. MIN, J. KIM, *Effects of hydrophobic surface on skin-friction drag*, Physics of Fluids, **16**, L55, 2004.

Received November 13, 2021; revised version February 15, 2022.
Published online April 24, 2022.